HEAT EXCHANGE CRISIS IN MESH STRUCTURES OF POWER PLANT EQUIPMENT

by

Alexander A. GENBACH[a], Hristo I. BELOEV[b], David Yu BONDARTSEV[a*], and Natalia A. GENBACH[a]

[a] Department of Heat and Power Units,
Almaty University of Power Engineering and Telecommunications, Almaty, Kazakhstan
[b] Agricultural Machinery Department, University of Ruse, Ruse, Bulgaria

Original scientific paper
https://doi.org/10.2298/TSCI210314305G

Thermal devices with porous structures, intended for the combustion chambers of gas turbine units, as well as for cutting and boring of the turbine housings of electric power plants have been developed and studied. Photographs of combustion chambers and nozzles, studied in terms of their geometry and thickening of the nozzle walls, excess oxidant (0.3-0.8) and the operating conditions until the limit state of the metal is reached ($1 \cdot 10^6$ W/m^2) have been presented. The optimal geometry of the chambers and nozzles, as well as the type of porous structure have been determined. Coolant consumption has been reduced dozens of times, which has environmental significance. The appraisal of the structures studied showed the advantages to the flow cooling system. An analytical model of the heat exchange crisis is proposed. The system of differential equations for 1-D flow of one-phase liquid is solved. A physical picture of the heat exchange process is presented. In the equation of motion, the coefficient which determines the viscosity in the general pressure gradient is introduced. The actual velocity of the fluid is accounted for by the coefficient of moisture content in the porous structure.

Key words*: capillary-porous structures, power plant, combustion chamber, nozzle, boiling crisis*

Introduction

In power plant equipment it is required to create a cooling system for high temperature parts and assemblies. These can include combustion chambers, nozzles and blades of gas turbine units, thermal instruments (tools) for construction and installation work. In cooling systems, bubbling fluid boiling processes take place. At high thermal loads a crisis situation with possible overheating of the heat exchange wall is probable. The design and fabrication of hybrid porous surfaces with a hybrid micro-nanoscale is of interest [1]. Rather topical are the ways to increase the efficiency of cooling combustion chambers and nozzles of gas turbines by different coolers, in order to achieve higher efficiency of the machines themselves and their cycles [2, 3]. Water, air and steam coolers are considered. We propose new integrated capillary-porous structures, which, unlike the existing ones, significantly increase the cycle efficiency of thermal power plants [4-7]. In Riadh and Platel [8] a complex 2-D model is built and numerical simulation of the actual problem of boiling crisis (formation of a *steam pocket*) of capillary loop in the wick is performed, taking into account mass forces. However, the authors

* Corresponding author, e-mail: d.bondartsev@aues.kz

have not conducted an experiment to confirm their model. Therefore, it is necessary for such complex heat transfer conditions to carry out experimental studies to identify critical loads and factors to control them. In [9-12], it is of interest to study the heat transfer of various homogeneous and heterogeneous porous coating surfaces (multi layers), as well as some specially designed wicks, in order to increase their heat transfer capacity. Studies have begun to appear [11, 12] of the thermohydraulic characteristics of boiling in porous media, using thermocouple measurements and observations with a high speed camera (bubble size, nucleation frequency and density). In Jamialahmadi *et al*. [13] the authors carry out a comparative analysis of methods for calculating heat transfer by boiling water with underheating in vertical channels, and consider focal corrosion of fuel element cladding of nuclear reactors as an analogue of capillary-porous structure. However, studies of heat transfer over a regular structured surface have not been conducted. In addition, the role of velocity and under-heating of liquid on the boiling crisis in capillary-porous coatings is not clear. The authors have studied profoundly enough the influence of the porous coating parameters, namely thickness [14-16], porosity and size of the particles, forming the capillary structure [17], and the geometry of this structure [18] on the boiling characteristics. Some works are devoted to the study of the influence of external conditions on the intensity of heat transfer during boiling, pressure in the system [19] and other factors [20]. However, all the aforementioned papers [1-3, 8-20] do not consider the combined effect of capillary and mass forces, and there is no connection between the bubble dynamics and the boiling curve in the porous medium.

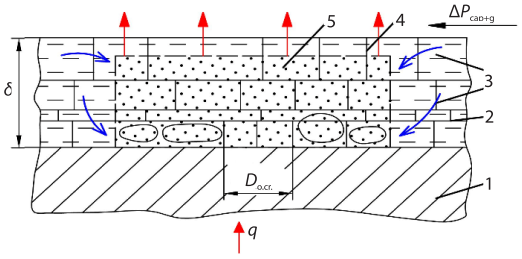

Figure 1. The onset of a boiling crisis in porous structures during the formation of a large steam mass (conglomerate), separated from the heating surface by a thin liquid layer with appearing *dry* spots: *1 – wall, 2 – porous structure, 3 – cooling liquid, 4 – steam front movement with its possible condensation in relatively cold liquid layers, and 5 – steam conglomerate*

Boiling crisis model

The model, fig. 1, has been developed for a new enhanced and highly intensive capillary-porous system of a new class of heat dissipation systems. The novelty is in the fact that the steam phase develops in a capillary-porous medium, where the capillary and mass potential work together. In this study, the mass force is the gravitational force $\rho_l \times g \times H$, where ρ_l is the liquid density, g – the free-fall acceleration, and H – the hydrostatic pressure, that is, the mass force arises as a result of the gravitational acceleration. Inertial mass forces arise from curvilinear or rotational motion of the coolant.

The excess cooling liquid $\tilde{m} = m_s/m_l$, located in the cross-section of the structure, F_w, and partly on its surface, creates an additional (forced) liquid velocity, as well as heating related to the saturated vapors temperature. Holography and high speed imaging have been used for the creation of the model [5]. The model developed considers the control over the heat transfer and the increase of this transfer due to the velocity and heating of the liquid-flow, q_{cr}. The boiling crisis model is presented as equations for continuity and movement, considering the combined action of gravitational and capillary forces, with the gravitational forces creating excess liquid $\tilde{m} = m_s/m_l$:

$$\frac{dV_y}{dy} = \frac{\rho_s L}{\rho_l \varepsilon F_w} V_x \left(\frac{m_s}{m_l} + 1 \right) \tag{1}$$

$$V_y \frac{\mathrm{d}V_y}{\mathrm{d}y} = \mathrm{g}\cos\beta + \frac{2\sigma}{\rho_l}\frac{\mathrm{d}}{\mathrm{d}y}\left(\frac{1}{R_{(y)}}\right) - \frac{\varepsilon \nu_l V_y}{K} \tag{2}$$

When substituting eq. (1) with eq. (2), considering the following values: $V_y = G_{l(y)}/\rho_l$, $V_x = q_{cr}/\rho_s$, and integrating the obtained in the range of $y_1 = 0$ to $y_2 = H$, and H and of $R_0 = \infty$, of up to $R_h = b_h/2$ we obtain:

$$\frac{3q_{cr}^2 h^2\left(\frac{m_s}{m_l}+1\right)}{2(r\varepsilon\delta_w\rho_l)^2\varphi'_{cr}} - \frac{3q_{cr}h^2\nu_l}{2r\varepsilon\delta_w\rho_l K\varphi'_{cr}} + \left(\mathrm{g}\cos\beta + \frac{2\sigma}{\rho_l R_h}\right) = 0 \tag{3}$$

The solution of the quadratic eq. (3) is an expression that determines the first critical heat flow of a slightly unheated and saturated liquid ($\tilde{m} \to 1$):

$$q_{cr} = \frac{[B \pm \left(B^2 - 4AC\right)^{0.5}]}{2A}, \quad \boldsymbol{A} = \frac{3h^2\left(\frac{m_s}{m_l}+1\right)}{2(r\varepsilon\delta_w\rho_l)^2\varphi'_{cr}},$$
$$\boldsymbol{B} = \frac{3h^2\nu_l}{2r\varepsilon\delta_w\rho_l K\varphi'_{cr}}, \quad \boldsymbol{C} = \mathrm{g}H\cos\beta + \frac{2\sigma}{\rho_l R_h} \tag{4}$$

Equation (4) determines the maximum height of the heat exchange surface, h, when a hydrodynamic crisis of heat exchange occurs. It eq. (4) does not contain specifically the m_s/m_l ratio, but it is considered through the values φ_{cr} and K. When $\varphi_{cr} \to 0$, the value $q_{cr} \to 0$, *i.e.* in the border layer of the porous structure, almost all moisture will evaporate and a boiling crisis will follow. The solution of eq. (4) concerning the height of the liquid column is of interest for both cases of liquid hydrodynamics: $K = K_{h,p}$ and $K = K_c$.

When all the liquid moves in the living section of the porous structure ($K = K_{h,p}$), it is required to create a sufficiently large pressure. For the cooling system studied, when: $h = (0.1...0.7)$, $\delta_w = (0.15...1.5) \cdot 10^{-3}$ m, $b_h = (0.08...1) \cdot 10^{-3}$ m, $\varphi'_{cr} = 0.1$ the value of H is dozens of meters of water column. In the second case, when excess liquid is created, during its free flow along the outer surface of the porous structure ($K = K_c$), the excess of the liquid column is dozens of millimeters. The condition $\rho_l gH \ll 2\sigma/R_h$ can be realized not only for horizontal lay-out of the cooling systems, but also when some of the liquid-flows along the outer surface of the porous structure ($K = K_c$). We should not conclude from eq. (4) that the value of $q_{cr.v}$, can be increased through an endless increase of hydrostatic pressure $\rho_l gH$ since in this case the value of K could lose the physical meaning of permeability because the main liquid-flow will be outside the living section of the structure, flowing freely on the porous material. Besides, with $q \le 6 \cdot 10^4$ W/m^2, heat taken through evaporation and convection will be redistributed to degeneration of the boiling process. With $q \to q_{cr.v}$, despite the large amount of liquid $G_l = F[H]$, crisis phenomena will occur, which will lead to burning and destruction of the heat exchange surface. In this case, for eq. (4) the inequality $\rho_l gH \gg 2\sigma/R_h$ will be met and it will be necessary to introduce the coefficient K/K_c. In the case when $\rho_l gH \approx 2\sigma/R_h$, and the value of $\Delta P_{cap+g} = (1.5...2) \times 2\sigma/R_h$, the value of H is tens of millimeters, depending on the structure thickness. The mass moisture content can vary from the moment the boiling starts ($\overline{\varphi}' \to 1$) to the boiling crisis ($\overline{\varphi}' = \varphi_{cr} \to 0.1$). The analysis conducted allows to determine the height of the heat exchange surface and the thickness of the porous structure, corresponding to the critical thermal load. Boiling in the porous body is considered, using the moisture content, $\overline{\varphi}'$, and the

parameter, which creates directed flow of the subcooled liquid at negligible velocity and makes it possible to ensure the stability of a two-phase flow in the boundary pulsating layer of the liquid. The evaluation of the temperature difference in the porous structure is needed for the stable operation of the cooling system. Such evaluation is rather complex because of the difficulty in determining the efficient coefficient of thermal conductivity at the moment of a boiling crisis, depending on numerous factors. The most essential of them are the presence of water-steam mixture in the boundary-layer, as well as contact resistance between the skeleton of the structure and the wall and between the elements of the skeleton itself. It can vary from the degree of compression of the structure to the wall and from the change in temperature level of operation, leading to thermal expansion of the mesh structure wires. Besides, in a crisis mode the thickness of the liquid layer is an indefinite value. The presence of a gravitational potential can expand the value of q_{cr} and stabilize the dependence $q_{cr} = f[\rho]$ for a wide range of pressure change (0.01... 20 MPa), which is particularly important when the system operates under high pressure. Moisture content $\bar{\varphi}'$ affects the value of q_{cr} through the ration $\bar{m}$ and the value $\bar{\varphi}'_{cr} = (0.1...0.15)$. Equation (4) is obtained on the basis of hydrodynamic analysis of the heat exchange processes, not taking into consideration the local restrictions of the thermal flow when the contact of the liquid film with the surface is impossible due to the strong overheating of this surface during the growth of the steam bubble.

The results from the experimental studies show that considering the hydrodynamic abilities of heat transfer is legitimate only in the presence of a liquid, exceeding (1.5...2) times the needed quantity, depending on the type of the structure. In addition, specific heat flows are introduced into the system, which are (2...8) times bigger than those in the heat pipes, when a mesh structure with bubble boiling is used. As most researchers note, for the heat pipes, the specific mass-flow of the liquid G_{cr} and V_{cr} is restricted by the capillary pressure limit value and determines the hydrodynamic boundary of the heat transfer capacity. In the system studied there is no such restriction. The value of G_{cr} is determined by the value of the acting pressure $\Delta P_{cap+g} = \rho_l g H + 2\sigma/R_{min}$.

For engineering calculations when taking specific heat flows to q_{cr}, with a developed boiling process, eq. (4) can be used. To do this, the pressure, the cooling system's geometry, and the type of porous structure must be known.

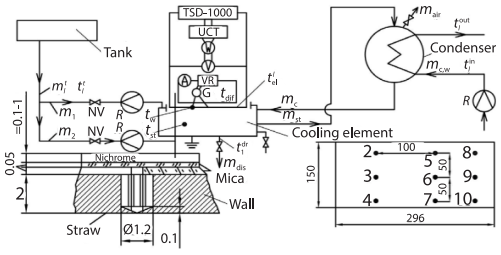

Figure 2. Operation scheme of a porous system and measurement technique: *TSD – welding transformer, UCT – universal current transformer, W – power meter, V – voltmeter, A – ammeter, VR – voltage regulator, G – galvanometer, R – rotameter, NV – needle valve*

Experimental conditions

In fig. 2 the operation scheme of porous cooling system, the technique of the measurement of heating surface temperature, t_{st}, and liquid consumption: m^t_l, m_1, m_2, m_{dis}, m_c, $m_{c.w}$, m_{air}, and steam m_{st} are shown. Accepted codes: t is the tank, dis – the discharge, c – the condensate, c.w. – the condensing water, and a – the air. Temperatures of liquid, t_w, t_l^t, t_l^{dr}, t_l^{out}, t_l^{in}, steam t_{st}, electrical insulation $t_{el}^i = t_{dif}$.

The supply of electrical energy to the main heater is carried out by a TSD type welding transformer, the output voltage of which has the following fixed values: 2.5, 5, 7.5, and 10 V. The electric current powering the heater is measured according to the scheme with

UCT-6M2 type class 0.2 universal transformer. The secondary current is up to 5 A, the primary current is 100-2000 A. The heater voltage drop is measured by a D523 class 0.5 voltmeter. The maximum possible error for the current measurement is ±0.6%, ±1% for voltage drop measurement, ±1.6% for power measurement. Electric energy is supplied to the guarding heater by a VR type voltage regulator. The TSD type current transformer, with 71 V no load output voltage, is used in studies at the start of liquid boiling and critical loads. The current strength is regulated within the limits of 200-1200 A. The measurements of liquid and environment temperatures are made using TL-4 mercury thermometers with 0-50 °C and 50-100 °C scale and division value of 0.1 °C. The temperatures of the drainage liquid and steam are measured by the Chromel-Copel thermocouples, made of wire $0.1 \cdot 10^{-3}$ m in diameter. The head diameter of the thermocouple junction is $0.4 \cdot 10^{-3}$ m. The thermocouple electrodes are isolated with dual channel straws with a diameter of $1 \cdot 10^{-3}$ m, that are attached with BF-2 glue inside the injection needles with diameter of $1.2 \cdot 10^{-3}$ m. The electrodes of the thermocouples with a diameter of $0.2 \cdot 10^{-3}$ m are welded to the wall by the electric arc, which is formed during the capacitors' discharge, to measure the temperature of the wall. In order to do that, drilling of the wall orthogonal to a surface with $2 \cdot 10^{-3}$ m thickness is carried out for $1.9 \cdot 10^{-3}$ m depth with the accuracy of $\pm 0.05 \cdot 10^{-3}$ m. The electrodes of the thermocouple are isolated with porcelain straws with $1.2 \cdot 10^{-3}$ m diameter and come out to the surface of the wall between two layers of mica with thickness of $0.05 \cdot 10^{-3}$ m attached to the surface of the heater. The cold ends of thermocouples are thermostated in melting ice. The electrodes of the thermocouple are connected with two PP-63 class 0.05 twelve-point switches. The installation and instruments are grounded to prevent the effect of induced wandering currents on indicated values of the thermocouple. The consumption of cooling and circulating liquid is determined by electric RED type rotameters with secondary electronic CSDH 43 class 1 type instruments, calibrated with volumetric method. The consumption of drained liquid and condensate are captured using a test measure with $0.5 \cdot 10^{-3}$ l pressure scale, and filling time with S-P-1b type stopwatch type with a 0.1 second division value [4].

The maximum possible error when determining liquid consumption by rotameters does not exceed ±3%, and by the volumetric method it is ±2%. The conditional permeance coefficient is further studied in [5]. The spread of K_c value when integrating experimental data does not exceed ±16%. The imbalance between heat supplied by current and heat, extracted by circulating and surplus water taking into account Q_{in}, does not exceed ±12%, and between heat supplied by steam in the condensing unit and heat, extracted by the circulating water does not exceed ±11%. The discrepancy of material balance between the consumption of cooling liquid, and that of drain and condensate is not more than ±10%. The measurements and the technique for processing of experimental data are published in the works [5].

Results from the experiment

Experimental studies were carried out up to the destruction of heaters and wicks of capillary-porous structures, fig. 3, as well as of combustion chambers and supersonic nozzles, fig. 4.

The structures are made of mesh with a hydraulic diameter $b_h = 0.4 \cdot 10^{-3}$ m. Some operational and technological abilities of the combustion chambers and nozzles until their destruction have been studied. Figure 2 shows combustion chambers of different lengths and nozzle outlet design: I-IV – $\alpha = 0.3$, V-VII – $\alpha = 0.65$-0.7, VIII – $\alpha = 0.8$; I-IV – porous cooling at $q_{cr.c\text{-}s.} = 5 \cdot 10^6$ W/m^2), and V-VIII – water cooling system at $q_{cr.c\text{-}s.} = 1 \cdot 10^6$ W/m^2.

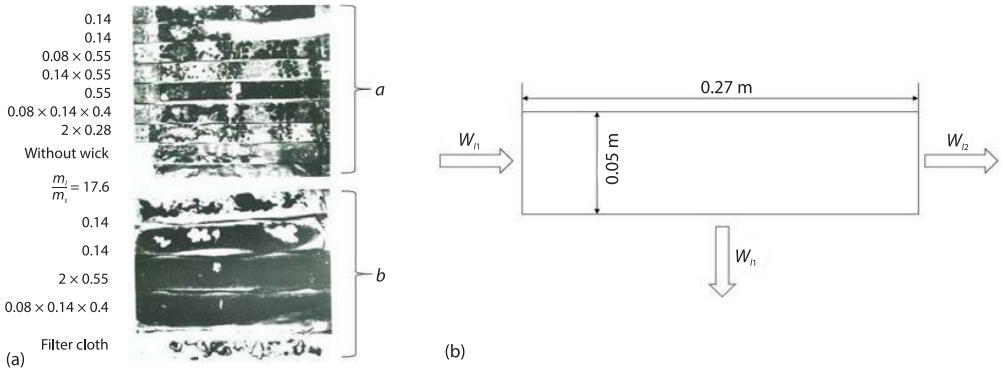

Figure 3. (a) General view of the limiting state of burned-out heaters – a and capillary-porous structures – b; the liquid excess varied from $m_s/m_l = 1$ to 17.6 and (b) fluid-flow diagram for fig. 3(a)

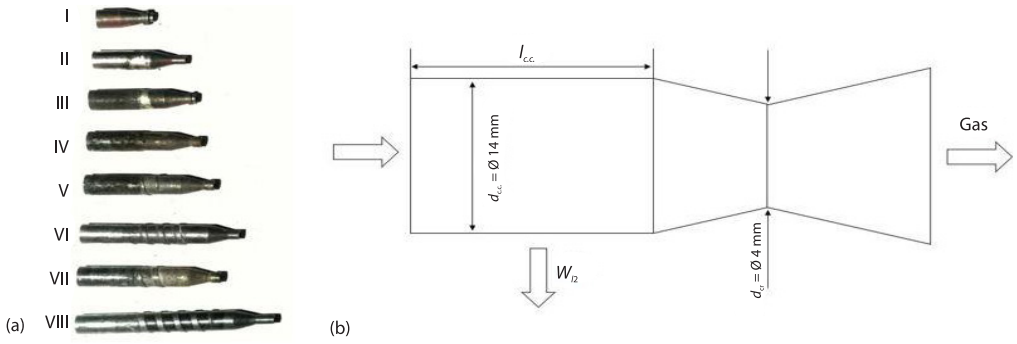

Figure 4. (a) General view of the experimental samples of combustion chambers and nozzles after operation and (b) diagram with indications on main constructional details and fluid-flows for fig. 4(a)

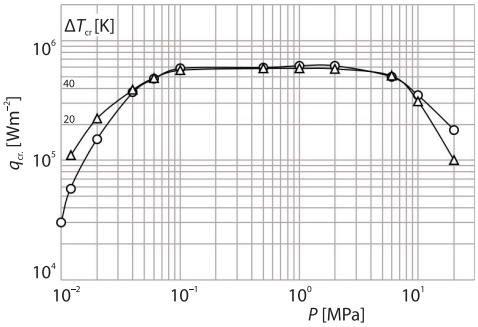

Figure 5. Effect of pressure, P, on the first critical heat flow, q_{cr}, and wall superheating, ΔT_{cr} – Δ, during water boiling in porous mesh structures: ○ - calculation by eq. (4); the mesh and wall are made of stainless steel. Experimental data (Δ, ○) were obtained at the following conditions: $h = 0.27$ m, $\tilde{m}$ = optimum, $H = 1$ m; $R_h = 0.275 \cdot 10^{-3}$ m, $\delta_w = 1.5 \cdot 10^{-3}$ m, and $\beta = 0°$

For cooling the heating surface of the combustion chambers and nozzles the following mesh-capillary structures have been used: $0.14 \cdot 10^{-3}$; $0.08 \times 0.55 \cdot 10^{-3}$; $0.14 \times 0.55 \cdot 10^{-3}$; $2 \times 0.55 \cdot 10^{-3}$; $0.08 \times 0.14 \times 0.4 \cdot 10^{-3}$;$2 \times 0.28 \cdot 10^{-3}$; $1 \times 1 \cdot 10^{-3}$, where the number shows the size of the mesh eye in mm. The porosity of the structure is approximately 70%. The maximum heat loads ($56 \cdot 10^4$ W/m^2) have been achieved for a mesh of $0.14 \cdot 10^{-3}$ m, $54 \cdot 10^4$ W/m^2 – for a two-layer mesh with eye size of $0.55 \cdot 10^{-3}$ m, $60 \cdot 10^4$ W/m^2 – for a mesh with an eye of $1 \cdot 10^{-3}$ m at optimal flow rate. To analyse the final limiting capacities q_{cr} of a porous energy and matter transmission system, it is necessary to determine from the equation q_{cr} the maximum height of the heat exchange surface h, in which a hydrodynamic heat exchange crisis will occur q_{cr} and $q_{cr.v}$, see fig. 5.

Discussion of the heat exchange crisis mechanism

The excess liquid $\tilde{m}$ in the porous system creates directed movement to the flow, V, which leads to the deformation of steam bubbles, reduces their diameter, and increases the frequency of their formation.

With the increase of flow velocity, V, increases the energy, used for moving the liquid from the boundary-layer closer to the wall. Therefore, the speed of steam generation, V_{cr}, and the value of q_{cr} increase as well. But at certain values of liquid-flow, determined by the parameter $\tilde{m}_{cr}$, the energy used for pushing the liquid out of the two-phased wall layer is insufficient and a heat exchange crisis occurs $q_{cr.v}$. Of course, the increase of $q_{cr.v}$ will be achieved at higher flow values. When a certain value of moisture consumption is reached $\overline{\varphi}'_{cr}$, the flow will not contribute to increasing the value of q_{cr}, and, in some cases, it can even lead to a decrease of q_{cr}, making it difficult to evacuate steam from the wall area. The increase of velocity of the liquid film adjacent to the wall, due to the parameter $\tilde{m}$, will start to give way to the dominant influence of the decline in moisture content $\overline{\varphi}'$ in the same area, which will affect to a large extent the value of q_{cr}, even reducing it. That is why, it is required to determine the optimal ratio of excess liquid $\tilde{m}$, depending on the porous structure. As a result of the imbalance of the acting forces, the quantity of incoming liquid becomes insufficient, *dry* spots appear on the heating surface K_{min}, the wall temperature gradually rises to a certain value and the process takes place at temperature pressure (60…80) K, and growing F_s/F. The pulsating mode of supplying liquid to the wall does not lead to burning of the surface although the intensity of heat transfer diminishes. However, there are pulsations in the wall temperature, causing thermal destructive pressure, which shortens the service life of the surface. That is why it is important to optimize the appearance of the porous structure and not to allow strong overheating of the wall, compared to the liquid temperature.

The best results have been achieved for a capillary-porous structure of the type 2×0.55, which allows to take out the largest heat flows with a combined action of mass and capillary forces. The structure, consisting of a single layer mesh $0.55 \cdot 10^{-3}$ m, forms a smaller stable liquid film on the surface, and, in case the number of mesh layers is more than two, the overheating of the wall increases considerably with respect to the steam temperature, which leads to an early occurrence of crisis phenomena. In addition, the increased pore size does not require a high degree of purification, as is the case with the heat pipes, and allows the use of water. The heat output of the proposed structure is six times as high as that achieved in the heat pipes and thin–layer evaporators. Burning of the wall occurs due to clogging of the mesh pores by steam bubbles, which hinders the flow of fresh doses of liquid to the heated pipe surface. If the wall does not contain a capillary-porous coating and the cooling is performed with a mixture of steam and water, when a thin liquid film is formed on the wall, this film decomposes into separate jets and drops at heat flows of about $1 \cdot 10^5$ W/m^2, which leads to burning of the wall. The liquid from the core of the moving water-steam flow does not move towards the heated surface, on whose inner side a continuous steam film is formed, the intensity of heat transfer deteriorates sharply. As a result, cyclic, sharply varying temperature stresses and disbalances occur, which worsens significantly the operating conditions of the heating surfaces until their destruction.

Conclusion

We demonstrated that the new porous structures reduce the likelihood of cracks in the nozzles and the combustion chambers. The porous systems allow the removal of powerful heat loads from the detonation high temperature jets, prevent the development of cracks, and are selected according to the cooling surface material properties. The capillary-porous and the flow

cooling systems demonstrate high efficiency to the border state of the combustion chambers and nozzles metal ($1 \cdot 10^6$ W/m^2), but the former has an environmental advantage. The results obtained can be extended to the modernisation of chimneys, and reinforced concrete cooling towers and operation is environmentally-friendly (the coolant consumption is reduced dozens of times). The optimised structured surfaces developed in the form of mesh structures yield an integrated effect of industrial mesh and possess the synergistic advantages of combining various structures in an integrated technology for their production through expanding the critical heat loads and controlling the border state of the heat exchange surface.

Nomenclature

b_h – hydraulic pore size and wick thickness, [m]
$D_{o,cr}$ – average size of a steam conglomerate that meets the condition $\Delta T=\Delta T_{cr}$, [m]
$d_{c,c}$. – combustion chamber diameter, [mm]
d_{cr} – critical nozzle diameter, [mm]
F, F_s – heating (cooling) surface and the surface covered with steam, [m^2]
F_w – section of the porous structure (wick), [m^2]
G_{cr} – critical specific liquid consumption, [kgm^{-2}s^{-1}]
$G_{l(y)}$ – specific liquid consumption, [kgm^{-2}s^{-1}]
g – acceleration of gravity, [ms^{-2}]
H – hydraulic head, [m]
h, L – height and the length of the heating surface, [m]
$l_{c,c}$ – variable combustion chamber length, [m]
K – coefficient of permeability, [m^2]
K_c – conditional coefficient of permeability, [m^2]
$K_{h,p}$ – permeability coefficient of the wicks of heat pipes (hp), [m^2]
K_{min} – coefficient, taking into account the presence of a dry spot under the steam bubble, [m^2]
m_l, m_s – liquid and steam flows, [kgs^{-1}]
$\tilde{m}$ – surplus of liquid (= m_s/m_l), [kgs^{-1}]
P – pressure, [Pa]
ΔP_{cap+g} – the total acting head (capillary and mass), [Pa]
q_{cr} – critical heat flow, [Wm^{-2}]
$q_{cr,c-s}$ – specific heat flux over a critical nozzle cross-section, [Wm^{-2}]
$q_{cr,v}$ – critical (limit) heat flow with liquid velocity V, [Wm^{-2}]
$R_{(y)}$ – radius of meniscus liquid, [m]
R_0 – radius measurement of liquid meniscus at the entry of the liquid, [m]
R_h – radius measurement of liquid meniscus at height h from the surface, [m]
R_{min} – minimum radius of meniscus liquid, [m]
r – heat of steam generation, [Jkg^{-1}]
T_w – temperatures walls, [K]
T_s – temperatures saturation, [K]
ΔT – temperature head (= $T_w - T_s$), [K or °C]
ΔT_{cr} – critical temperature head, [K]
V – velocity, [ms^{-1}]
V_x – steam velocity by co-ordinate x, [ms^{-1}]
V_y – liquid velocity by co-ordinate y, [ms^{-1}]
V_{cr} – critical steam velocity, [ms^{-1}]
v_l – coefficient of kinetic viscosity of the liquid, [m^{2}s^{-1}]
W_l – velocity of the gas [ms^{-1}]

Greek symbols

α – excess air factor
β – angle of the slope of cooling system to the vertical line, [°]
δ_w – wick thickness, [m]
ε – porosity
ρ – density, [kgm^{-3}]
ρ_l, ρ_s – liquid and steam density, [kgm^{-3}]
σ – coefficient of surface tension, [Nm^{-1}]
$\overline{\varphi}'$ – consumption liquid content
$\overline{\varphi}'_{cr}$ – critical consumption liquid content

References

[1] Shoukat, A. K., *et al*., Design, Fabrication and Nucleate Pool-Boiling Heat Transfer Performance of Hybrid Micro-Nanoscale 2-D Modulated Porous Surfaces. *Applied Thermal Engineering*, *153* (2019), May, pp. 168-180
[2] Wei, W., *et al.*, Cooling Performance Analysis of Steam Cooled Gas Turbine Nozzle Guide Vane. *International Journal of Heat and Mass Transfer*, 62 (2013), July, pp. 668-679
[3] Xing, Y., *et at*., Turbine Platform Phantom Cooling from Airfoil Film Coolant, with Purge Flow. *International Journal of Heat and Mass Transfer*, *140* (2019), Sept., pp. 25-40
[4] Genbach, A. A., *et al*., Heat Transfer Crisis in the Capillary-Porous Cooling System of Elements of Heat and Power Installations, *Thermal Science*, *23* (2019), 2, pp. 849-860

[5] Genbach, A. A., *et al*., Scientific Method of Creation of Ecologically Clean Capillary-Porous Systems of Cooling of Power Equipment Elements of Power Plants on the Example of Gas Turbines, *Energy*, *199* (2020), 117458
[6] Genbach A. A., Bondartsev, D. Y., Limiting Thermal State of Capillary-Porous Power-Plant Components, *Russian Engineering Research*, *40* (2020), 5, pp. 384-389
[7] Genbach, A., *et al*., A Study of Thermal Devices with Porous Coatings, 2021 IOP Conf. Ser.: *Mater. Sci. Eng*., *1032* (2021), 012039
[8] Riadh, B., Platel, V., Dynamic Model of Capillary Pumped Loop with Unsaturated Porous Wick for Terrestrial Application, *Energy*, *111* (2016), Sept., pp. 402-413
[9] Poniewski, M. E., Peculiarities of Boiling Heat Transfer on Capillary-Porous Coverings. *International Journal of Thermal Sciences*, *43* (2004), 5, pp. 431-442
[10] Odagiri, K., Hosei Nagano, H., Investigation on Liquid-Vapor Interface Behavior in Capillary Evaporator for High Heat Flux Loop Heat Pipe, *International Journal of Thermal Sciences*, *140* (2019), June, pp. 530-538
[11] Chang, Y. M., Ferng, Y. H., Experimental Investigation on Bubble Dynamics and Boiling Heat Transfer for Saturated Pool Boiling and Comparison Data with Previous Works, *Applied Thermal Engineering*, *154* (2019), 25, pp. 284-293
[12] Chuang, T. J., *et al.*, Investigating Effects of Heating Orientations on Nucleate Boiling Heat Transfer, Bubble Dynamics, and Wall Heat Flux Partition Boiling Model for Pool Boiling, *Applied Thermal Engineering*, *163* (2019), 25, 114358
[13] Jamialahmadi, M., *et at*., Experimental and Theoretical Studies on Subcooled Flow Boiling of Pure Liquids and Multicomponent Mixtures, *International Journal of Heat and Mass Transfer*, *51* (2008), 9-10, pp. 2482-2493
[14] Alam, M. S., *et al*., Enhanced Boiling of Saturated Water on Copper Coated Heating Tubes, *Chemical Engineering and Processing: Process Intensification*, *47* (2008), 1, pp. 159-167
[15] Chen, L., *et al*., Evaporation/Boiling in Thin Capillary Wicks (l) – Wick Thickness Effects. *Journal of Heat Transfer*, *128* (2006), 12, pp. 1312-1319
[16] Hanlon, M. A., Ma, H. B., Evaporation Heat Transfer in Sintered Porous Media. *Journal of Heat Transfer*, *125* (2003), 4, pp. 644-652
[17] Chen, L., Peterson, G. P., Evaporation/Boiling in Thin Capillary Wicks (II) – Effects of Volumetric Porosity and Mesh Size. *Journal of Heat Transfer*, *128* (2006), 12, pp. 1320-1328
[18] Das, A. K., *et al.*, Performance of Different Structured Surfaces in Nucleate Pool Boiling, *Applied Thermal Engineering*, *29* (2009), 17-18, pp. 3643-3653
[19] Arik, M., *et al*., Enhancement of Pool Boiling Critical Heat Flux in Dielectric Liquids by Microporous Coatings, *International Journal of Heat and Mass Transfer*, *50* (2007), 5-6, pp. 997-1009
[20] Sohail, M. S., *et al*., Subcooled flow Boiling CHF Enhancement with Porous Surface Coatings. *International Journal of Heat and Mass Transfer*, *50* (2007), 17-18, pp. 3649-3657

Paper submitted: March 14, 2021
Paper revised: August 28, 2021
Paper accepted: September 9, 2021